Inorganic Chemistry

pubs.acs.org/IC

Communication

Mechanisms of Luminescence in Lanthanide Complexes: A Crucial Role of Metal−Ligand Covalency

Liviu Ungur,* Bernat Szabo, Zeid A. ALOthman, Abdullah A. S. Al-Kahtani, and Liviu F. Chibotaru*

Cite This: *Inorg. Chem.* 2022, 61, 5972−5976

Read Online

ACCESS | Metrics & More | Article Recommendations | Supporting Information

ABSTRACT: A current understanding of the luminescence of lanthanide complexes is based on the phenomenological Judd−Ofelt (JO) theory. However, the mechanisms of electric-dipole transitions lying at its basis were never subjected to a rigorous analysis. Here, we investigate the contributions to the electric-dipole transitions in the Er^{3+} $^4S_{3/2} \rightarrow {}^4I_{15/2}$ band of an erbium trensal complex using state-of-the-art *ab initio* calculations. We find that the conventional JO mechanism based on the electrostatic crystal field yields only a quarter of the integral intensity of this band. Accordingly, three quarters of it is contributed by covalent binding of erbium and ligand orbitals via three major mechanisms, the 4f ligand and ligand−ligand electric-dipole transitions and covalent enhancement of the hybridization of 4f and even empty orbitals of erbium. We expect that these findings will inspire the design of efficient rare-earth luminescent materials.

Optical spectroscopy of rare-earth ions or lanthanide (Ln) ions[1,2] is a continuously active research topic first and foremost because of numerous current applications.[3−9] Thus, rare earths often serve as hybrid materials[10−12] and agents in magnetoresonance imaging[13] and are widely used in lasers and optical amplifiers,[1,2,14−16] for upconversion luminescence,[17,18] in a variety of near-field optical sensors, and as phosphors, in particular, in display screens.[19] The sharp and intense luminescence displayed by Ln ions in various environments is due to strongly differing angular momentum quantum numbers of the involved multiplets, their weak crystal-field (CF) splitting, and a very weak electron-vibrational coupling for 4f electrons resulting in strongly suppressed radiationless transitions.[20] The description of the integral intensity (II) of luminescence has been done for decades within the phenomenological Judd−Ofelt (JO) theory.[21,22] However, the mechanism of the optical transition incorporated in this theory has never been subjected to rigorous analysis.

According to the Laporte selection rule,[23,24] electronic transitions that conserve parity are forbidden. Then electric-dipole transitions between multiplets built on molecular orbitals (MOs) of the 4f type will only be allowed if the nearest environment lacks inversion symmetry. Judd and Ofelt assumed that violation of the Laporte rule in such environments is via an electrostatic crystal field (ECF) admixture of Ln orbitals of even parity (5d, 4g, etc.) to the 4f orbitals.[21,22] On the other hand, it is well-known that metal−ligand covalency can also contribute to splitting of the Ln 4f shell,[25,26] which gives rise to a "covalent" version of the CF theory, the angular overlap model (AOM).[27−29] Both ECF and AOM are phenomenological approaches describing (i.e., fitting) the experiment with comparable accuracy that did not allow for a long time to elucidate the actual role of electrostatic and covalent contributions to the CF in rare earths. Recently, when high-level *ab initio* calculations were applied, the two contributions were found to be roughly equal in strength in the erbium trensal complex.[30] Despite its efficiency for the description of the electronic structure, magnetism, CF,[20,30] and $4f^{N-1}$−$4f^N5d^1$ optical transitions,[31] the *ab initio* approach has not been applied yet to analysis of the mechanisms driving the luminescence of Ln ions.

Here we report explicitly correlated *ab initio* calculations[32,33] of rare-earth luminescence and the investigation of possible mechanisms of the electric-dipole transitions. We chose to analyze the Er^{3+4} $S_{3/2} \rightarrow {}^4I_{15/2}$ green emission band of the erbium trensal complex[34,35] (Figure 1) because of a successful previous investigation of its CF spectrum by the same method.[30] Besides, the green emission band of Er^{3+} is famous for its use in the optical amplification of information signals in telecommunications optical fiber networks.[14−16]

The molecular terms of erbium trensal were calculated with the complete-active-space self-consistent-field (CASSCF) method,[36,37] as implemented in the *MOLCAS* package.[32,33] The experimental structure determined at 293 K was employed.[38] The Er, O, N, and C atoms close to Er were described by ANO-RCC-VDZP/VTZP basis sets; the more distant C and H atoms were described by the same basis set without polarization. The active space of CASSCF included only electrons spanning seven 4f orbitals of the Er^{3+} ion. In the second step, spin−orbit coupling was taken into account within the space of the calculated terms in the atomic mean-field approximation[39] using the RASSI module of MOLCAS.[32,33,40] The obtained spin−orbit multiplets of the complex were used for calculation of the intensities (rates of

Received: January 8, 2022
Published: April 14, 2022

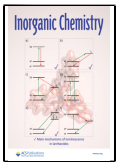

https://doi.org/10.1021/acs.inorgchem.2c00071
Inorg. Chem. 2022, 61, 5972−5976

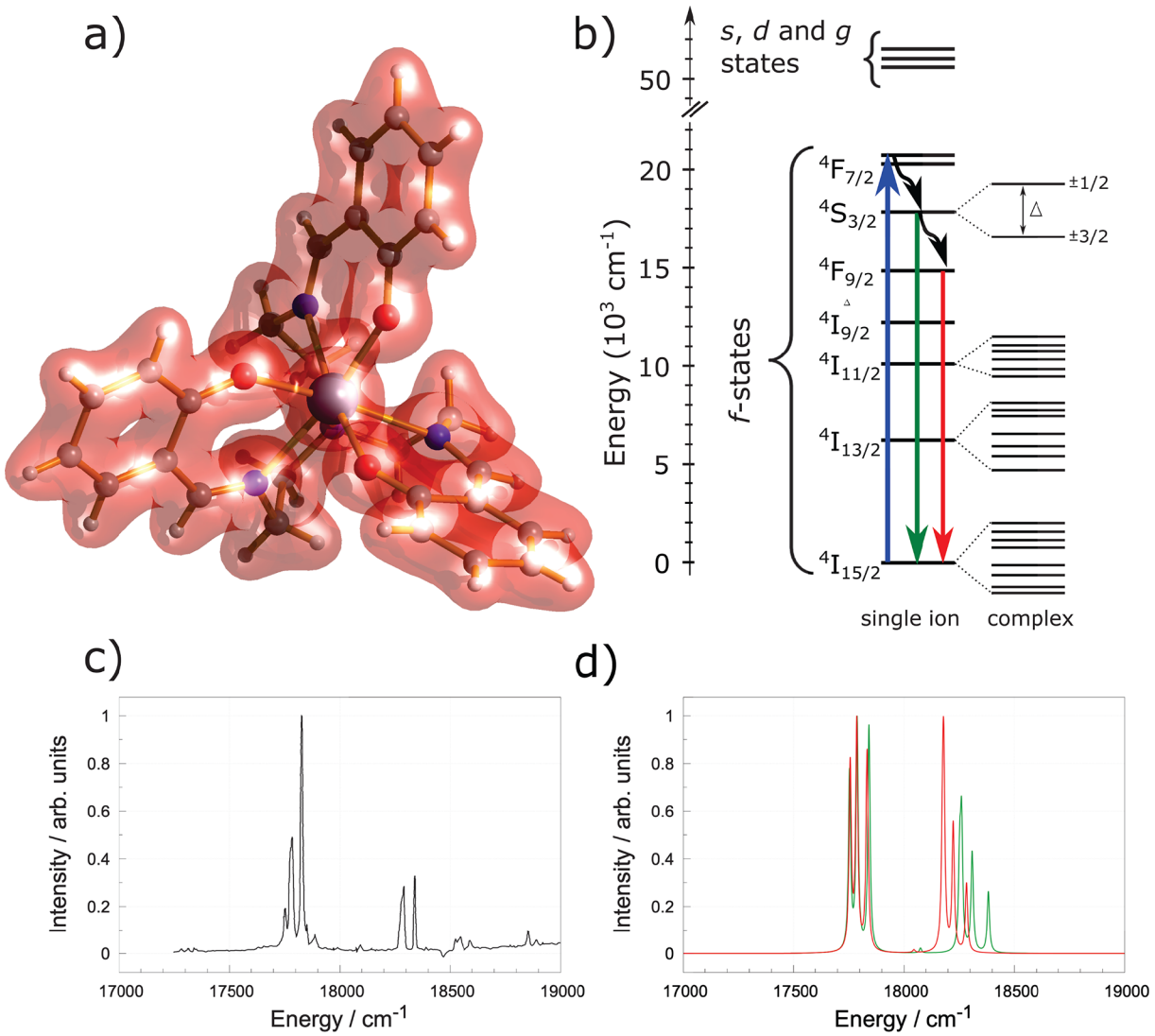

Figure 1. (a) View of erbium trensal with the electronic density distribution at the $(trensal)^{3-}$ ligand surrounding Er^{3+} (pink ground). (b) Electronic transitions involved in the luminescence of a Er^{3+} ion: optical pumping (blue) green and red (not considered here) emission and radiationless transitions (wavy arrows). (c) Measured profile of the $^4S_{3/2} \rightarrow {}^4I_{15/2}$ emission band of erbium trensal. Reproduced with permission from ref 34. Copyright 2001 American Chemical Society. (d) Calculated spectrum within the VDZP (green line) and VTZP (red line) basis sets.

spontaneous emission) of electric-dipole transitions within the green emission band (Figure 1b). The calculated spectrum reproduces the main features of this band (Figure 1d).

The II of this band taken as a sum of the rates of spontaneous emission of the corresponding optical transitions per molecule amounted to 4253 and 3901 s^{-1} for calculations within the VDZP and VTZP basis sets, respectively. In order to assess the role of erbium ligand covalency in the observed II, we made another series of similar calculations in which complete quenching of hybridization between the erbium and ligand orbitals is achieved via application of the fragment *ab initio* model potential approach.[41] These calculations basically describe an ECF splitting of erbium multiplets (including those arising from the 4f shell) of the Er^{3+} ion in a self-consistent field of the electron distribution of the ligand (Figure 1a).[30] The results are shown in the first column of Table 1, from which we may conclude that quenching of the erbium ligand covalency drastically reduces the II to 26% (VDZP) and 23% (VTZP) with respect to their values in the conventional *ab initio* calculation of the complex.

Table 1. Integral Intensity of the Green Band Arising from ECF (s^{-1})

basis set	full	no 5d	no empty even	no empty odd
VDZP	1094	16	0	1320
VTZP	908	32	0	1356

Further insight is obtained by specifying possible electric dipolar mechanisms of luminescence in terms of atomic-like orbitals. The optical transitions between 4f multiplets in a Ln complex arise via nonzero matrix elements of electric dipolar momentum (**D**) on constituting MOs of the 4f type. To this end, the hybridization of atomic 4f orbitals with all other orbitals in the complex is essential and can be written in symbolic form:

$$\psi_{4f} = \tilde{c}_{4f}\varphi_{4f} + \tilde{c}_{5d}\tilde{\varphi}_{5d} + \tilde{c}_{6p}\tilde{\varphi}_{6p} + \tilde{c}_{L}\tilde{\varphi}_{L} \quad (1)$$

where φ_{4f} is a normalized combination of seven atomic 4f (Ln) orbitals, $\tilde{\varphi}_{5d}$ and $\tilde{\varphi}_{6p}$ are orbitals originating from even (e.g., 5d) and odd (e.g., 6p) empty Ln orbitals, and $\tilde{\varphi}_{L}$ denotes

https://doi.org/10.1021/acs.inorgchem.2c00071
Inorg. Chem. 2022, 61, 5972−5976

ligand-type orbitals. The hybridization is usually weak ($c_{4f} \approx 1$), whereas the tilded orbitals are characterized by a much stronger covalent hybridization with other non-4f atomic orbitals (AOs), e.g.

$$\tilde{\varphi}_{5d} = \tilde{\alpha}_{5d5d}\varphi_{5d} + \tilde{\alpha}_{5dL}\varphi_{L} + \tilde{\alpha}_{5d6p}\varphi_{6p} \quad (2)$$

with the α coefficients of similar order of magnitude for all AOs. φ_{5d} and φ_{6p} represent the group of excited (empty) atomic Ln orbitals of even and odd parity, respectively, whereas φ_{L} denotes the net ligands' orbitals (see the Supporting Information). The expression for the electric dipolar matrix element on two MOs of the 4f type, $\langle\psi_{4f}|\mathbf{D}|\psi'_{4f}\rangle$, after the substitution of eq 2 into eq 1 displays six distinct contributions in terms of the Ln AOs and ligands' MOs (eqs S7−S9), which give rise to six mechanisms of electric dipolar transitions in Ln ions (Figure 2). These comprise two two-step mechanisms (plots a and b) and four three-step ones (plots c−f).

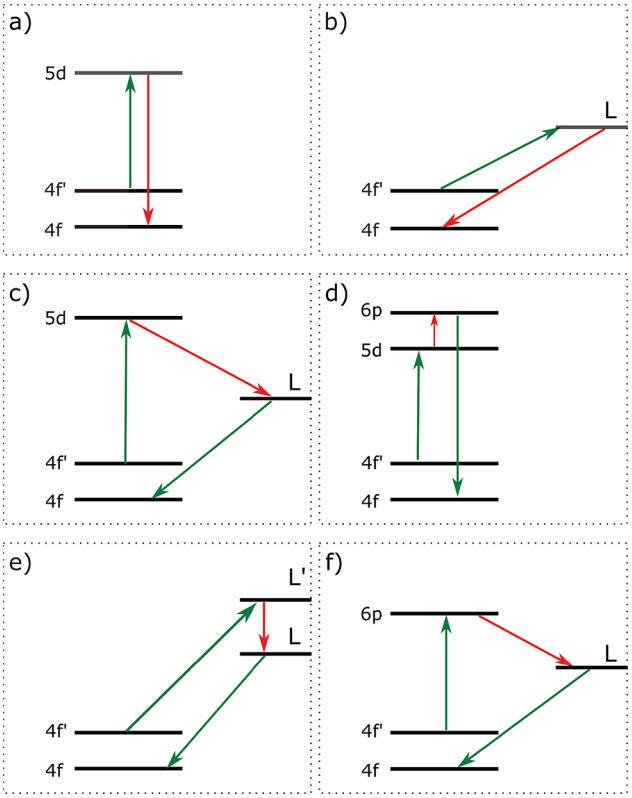

Figure 2. Six mechanisms of electric dipolar transitions between 4f orbitals in Ln complexes. Red arrows stand for electric dipolar coupling, and green arrows denote covalent (when relevant) and ECF admixtures of excited Ln and ligand orbitals. As stated in the text, the label "5d" in the above scheme stands for "all even empty orbitals of the lanthanide" and label "6s" stands for "all odd empty orbitals of the lanthanide".

Assessment of the strength of each of the six mechanisms is achieved via consequent quenching in calculations of the intensity of the electric dipolar matrix elements between all AOs except those connected by red arrows in the corresponding mechanism in Figure 2. One should note that the overall II (corresponding to the full calculation) is by far not a simple sum of partial contributions from the six mechanisms because of their interference in the individual matrix elements $\langle\psi_{4f}|\mathbf{D}|\psi'_{4f}\rangle$ (eq S4).

In terms of these mechanisms, the partial contribution to the II in the last column of Table 1 corresponds to (a), i.e., to the conventional JO mechanism; all other contributions entail, in addition, the mechanism (d). Because suppression of the latter significantly changes the results of the full calculation, we may conclude that the contribution of electric-dipole transitions between even (5d) and odd (6p) empty Ln AOs, originally not considered by Judd and Ofelt,[21,22] is by far nonnegligible. This may come as a surprise given that (d) is a three-step mechanism, i.e., containing an additional small factor ($\tilde{c}_{6p}$ or $\tilde{c}_{5d}$; eq 1) in the expression for the electric dipolar matrix element $\mathbf{D}^{(d)}$ (eq S9) compared to the two-step transition $\mathbf{D}^{(a)}$ corresponding to the JO mechanism (eq S8). One should keep in mind, however, a stronger ECP admixture of the odd erbium orbitals to the 4f ones, a larger number of transitions involved in mechanism (d), and larger electric dipolar matrix elements compared to those in mechanism (a). As shown in the second column of Table 1, the major contribution to the ECP luminescence, in particular to the JO mechanism, is provided by the admixture of the Er 5d orbitals. Given the larger II due to the JO mechanism alone (last column in Table 1), we may conclude that the addition of mechanism (d) results in a negative interference with the former, leading to diminishing luminescence (first column).

Next we investigate the strengths of the luminescence mechanisms in Figure 2 on the basis of full *ab initio* calculation. The six distinct contributions to the II are listed in Table 2. We

Table 2. Contributions to the Integral Intensity from the Six Electric-Dipole Mechanisms in Figure 2 (cm^{-1})

basis set	(a)	(b)	(c)	(d)	(e)	(f)
VDZP	3221	2307	688	308	1475	427
VTZP	3249	1760	161	66	1645	145

can see that the JO mechanism (a) is enhanced several times compared to the ECP description (last column in Table 1) and now alone amounts to almost the entire II. The reason for that is the strongly increased hybridization between the 4f and even erbium orbitals via their mutual covalent admixture to the ligand orbitals. The effect of this admixture is especially strong for the empty erbium orbitals, as shown in Figure 3.

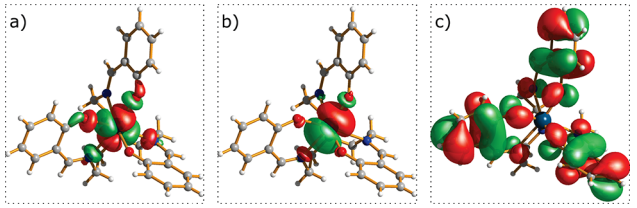

Figure 3. Representative "non-4f" MOs of erbium trensal contributing to ψ_{4f} (eq 1): (a) LUMO $\tilde{\varphi}_{5d}$; (b) LUMO $\tilde{\varphi}_{6p}$; (c) HOMO $\tilde{\varphi}_{L}$.

Comparable II magnitudes are provided by mechanisms (b) and (e), both arising from the 4f ligand covalency effects. Analysis of the contributions of empty and occupied erbium orbitals, relevant for all mechanisms except (b) and (e), shows that the former are by far the dominant ones.

In summary, a decent description of the multiplets of the erbium trensal complex[30] enabled a realistic estimation of

https://doi.org/10.1021/acs.inorgchem.2c00071
Inorg. Chem. 2022, 61, 5972−5976

relative contributions to the II of its green emission band from six possible mechanisms of electric-dipole transitions. It is found that the contribution from the conventional JO mechanism based on the ECF constitutes only a small fraction of the II, the main part arising from erbium ligand covalency through the 4f ligand and ligand−ligand electric-dipole transitions, and covalent enhancement of the hybridization of 4f and the even empty erbium orbitals. Hence, increasing the Ln ligand covalency represents the major route toward highly luminescent Ln materials.

■ ASSOCIATED CONTENT

Supporting Information

The Supporting Information is available free of charge at https://pubs.acs.org/doi/10.1021/acs.inorgchem.2c00071.

Ab initio calculation of luminescence, electric dipolar matrix element in terms of AOs, and mechanisms of the electric-dipole transitions (PDF)

■ AUTHOR INFORMATION

Corresponding Authors

Liviu Ungur − *Department of Chemistry, National University of Singapore, Singapore 117543, Singapore;* orcid.org/0000-0001-5015-4225; Email: chmlu@nus.edu.sg

Liviu F. Chibotaru − *Theory of Nanomaterials Group, Katholieke Universiteit Leuven, Leuven B-3001, Belgium; Chemistry Department, College of Science, King Saud University, Riyadh 11451, Saudi Arabia;* orcid.org/0000-0003-1556-0812; Email: Liviu.Chibotaru@kuleuven.be

Authors

Bernat Szabo − *Theory of Nanomaterials Group, Katholieke Universiteit Leuven, Leuven B-3001, Belgium;* orcid.org/0000-0003-1824-8322

Zeid A. ALOthman − *Chemistry Department, College of Science, King Saud University, Riyadh 11451, Saudi Arabia;* orcid.org/0000-0001-9970-2480

Abdullah A. S. Al-Kahtani − *Chemistry Department, College of Science, King Saud University, Riyadh 11451, Saudi Arabia*

Complete contact information is available at: https://pubs.acs.org/10.1021/acs.inorgchem.2c00071

Notes

The authors declare no competing financial interest.

■ ACKNOWLEDGMENTS

L.U. acknowledges financial support of Research Projects R-143-000-A65-133, R-143-000-A80-114 and A-8000017-00-00 of the National University of Singapore. *Ab initio* calculations were done on the ASPIRE-1 cluster (www.nscc.sg) under Project 11001278. This work was supported by the Distinguished Scientist Fellowship Program of King Saud University, Riyadh, Saudi Arabia.

■ REFERENCES

(1) Hüfner, S. *Optical Spectra of Transparent Rare Earth Compounds*; Academic Press: New York, 1978.

(2) Henderson, B.; Imbusch, G. F. *Optical Spectroscopy of Inorganic Solids*; Oxford University Press: Oxford, U.K., 1989.

(3) Reisfeld, R. Optical Properties of Lanthanides in Condensed Phase, Theory and Applications. *AIMS Mater. Sci.* **2015**, *2*, 37.

(4) Bünzli, J.-C. G. Including Actinides. In *Handbook on the Physics and Chemistry of Rare Earths*; Bünzli, J.-C. G., Pecharsky, V. K., Eds.; Elsevier, 2016; Vol. *50*; pp 141−176.

(5) Bünzli, J.-C. G.; Comby, S.; Chauvin, A.-S.; Vandevyver, C. D. B. New Opportunities for Lanthanide Luminescence. *J. Rare Earths* **2007**, *25*, 257−274.

(6) Xia, Z.; Meijerink, A. Ce3+-Doped garnet phosphors: composition modification, luminescence properties and applications. *Chem. Soc. Rev.* **2017**, *46*, 275−299.

(7) Joos, J. J.; Van der Heggen, D.; Amidani, L.; Seijo, L.; Barandiarán, Z. Elucidation of the electron transfer mechanism in Eu^{2+} and Sm^{3+} codoped CaF_2: A step towards better understanding of trapping and detrapping in luminescent materials. *Phys. Rev. B* **2021**, *104*, L201108.

(8) Wu, S.; Min, H.; Shi, W.; Cheng, P. Multicenter Metal-Organic Framework-Based Ratiometric Fluorescent Sensors. *Adv. Mater.* **2020**, *32*, 1805871.

(9) Zhang, K. Y.; Yu, Q.; Wei, H.; Liu, S.; Zhao, Q.; Huang, W. Long-Lived Emissive Probes for Time-Resolved Photoluminescence Bioimaging and Biosensing. *Chem. Rev.* **2018**, *118*, 1770−1839.

(10) Binnemans, K. Lanthanide-Based Luminescent Hybrid Materials. *Chem. Rev.* **2009**, *109*, 4283−4374.

(11) Rocha, J. a.; Carlos, L. D.; Paz, F. A. A.; Ananias, D. Luminescent multifunctional lanthanides-based metal−organic frameworks. *Chem. Soc. Rev.* **2011**, *40*, 926−940.

(12) Schoenes, J. Magneto-optic lanthanide materials1Invited Paper presented at the 21 st Rare Earth Research Conference, Duluth, MN, USA, July 7−12, 19961. *J. Alloys Compd.* **1997**, *250*, 627−634.

(13) Bottrill, M.; Kwok, L.; Long, N. J. Lanthanides in magnetic resonance imaging. *Chem. Soc. Rev.* **2006**, *35*, 557−571.

(14) Becker, P. C.; Olsson, N. A.; Simpson, J. R. *Erbium-Doped Fiber Amplifiers: Fundamentals and Technology*; Academic Press: San Diego, CA, 1999.

(15) Graydon, O.; Loh, W.; Laming, R.; Dong, L. Triple-frequency operation of an Er-doped twincore fiber loop laser. *IEEE Photon. Technol. Lett.* **1996**, *8*, 63−65.

(16) Poole, S.; Payne, D.; Mears, R.; Fermann, M.; Laming, R. Fabrication and characterization of low-loss optical fibers containing rare-earth ions. *J. Light. Technol.* **1986**, *4*, 870−876.

(17) Bünzli, J.-C. G.; Eliseeva, S. V. Lanthanide NIR luminescence for telecommunications, bioanalyses and solar energy conversion. *J. Rare Earths* **2010**, *28*, 824−842.

(18) Wang, F.; Liu, X. Recent advances in the chemistry of lanthanide-doped upconversion nanocrystals. *Chem. Soc. Rev.* **2009**, *38*, 976−989.

(19) Aigouy, L.; Lalanne, P.; Hugonin, J. P.; Julié, G.; Mathet, V.; Mortier, M. Near-Field Analysis of Surface Waves Launched at Nanoslit Apertures. *Phys. Rev. Lett.* **2007**, *98*, 153902.

(20) Ungur, L. Advanced Nanomaterials. In *Lanthanide-Based Multifunctional Materials*; Martín-Ramos, P., Ramos Silva, M., Eds.; Elsevier, 2018; pp 1−58.

(21) Judd, B. R. Optical Absorption Intensities of Rare-Earth Ions. *Phys. Rev.* **1962**, *127*, 750−761.

(22) Ofelt, G. S. Intensities of Crystal Spectra of Rare-Earth Ions. *J. Chem. Phys.* **1962**, *37*, 511−520.

(23) Wybourne, B. G. *Spectroscopic Properties of Rare Earths*; John Wiley & Sons: New York, 1965.

(24) Laporte, O.; Meggers, W. F. Some Rules of Spectral Structure. *J. Opt. Soc. Am.* **1925**, *11*, 459−463.

(25) Jørgensen, C. K.; Pappalardo, R.; Schmidtke, H. Do the "Ligand Field" Parameters in Lanthanides Represent Weak Covalent Bonding? *J. Chem. Phys.* **1963**, *39*, 1422−1430.

(26) Watson, R. E.; Freeman, A. J. Covalent Effects in Rare-Earth Crystal-Field Splittings. *Proteins* **1967**, *156*, 251−258.

(27) Schäffer, C. E.; Jørgensen, C. K. The angular overlap model, an attempt to revive the ligand field approaches. *Mol. Phys.* **1965**, *9*, 401−412.

(28) Urland, W. On the ligand-field potential for f electrons in the angular overlap model. *Chem. Phys.* **1976**, *14*, 393−401.

(29) Figgis, B. N.; Hitchman, M. A. *Ligand Field Theory and Its Applications*; Wiley-VCH, 1999.
(30) Ungur, L.; Chibotaru, L. F. Ab Initio Crystal Field for Lanthanides. *Chem. Eur. J.* **2017**, *23*, 3708−3718.
(31) Munoz-Garcia, A. B.; Pascual, J. L.; Barandiaran, Z.; Seijo, L. Structural effects and 4f-5d transition shifts induced by La codoping in Ce-doped yttrium aluminum garnet: First-principles study. *Phys. Rev. B* **2010**, *82*, 82.
(32) Aquilante, F.; et al. Molcas 8: New capabilities for multiconfigurational quantum chemical calculations across the periodic table. *J. Comput. Chem.* **2016**, *37*, 506−541.
(33) Aquilante, F.; et al. Modern quantum chemistry with [Open]Molcas. *J. Chem. Phys.* **2020**, *152*, 214117.
(34) Flanagan, B. M.; Bernhardt, P. V.; Krausz, E. R.; Lüthi, S. R.; Riley, M. J. Ligand-Field Analysis of an Er(III) Complex with a Heptadentate Tripodal N_4O_3 Ligand. *Inorg. Chem.* **2001**, *40*, 5401−5407.
(35) Flanagan, B. M.; Bernhardt, P. V.; Krausz, E. R.; Lüthi, S. R.; Riley, M. J. A Ligand-Field Analysis of the trensal (H3trensal = 2,2‘,2“-Tris(salicylideneimino)triethylamine) Ligand. An Application of the Angular Overlap Model to Lanthanides. *Inorg. Chem.* **2002**, *41*, 5024−5033.
(36) Siegbahn, P. E. M.; Almlöf, J.; Heiberg, A.; Roos, B. O. The complete active space SCF (CASSCF) method in a Newton−Raphson formulation with application to the HNO molecule. *J. Chem. Phys.* **1981**, *74*, 2384−2396.
(37) Olsen, J.; Roos, B. O.; Jørgensen, P.; Jensen, H. J. A. Determinant based configuration interaction algorithms for complete and restricted configuration interaction spaces. *J. Chem. Phys.* **1988**, *89*, 2185−2192.
(38) Pedersen, K. S.; Ungur, L.; Sigrist, M.; Sundt, A.; Schau-Magnussen, M.; Vieru, V.; Mutka, H.; Rols, S.; Weihe, H.; Waldmann, O.; Chibotaru, L. F.; Bendix, J.; Dreiser, J. Modifying the properties of 4f single-ion magnets by peripheral ligand functionalisation. *Chem. Sci.* **2014**, *5*, 1650−1660.
(39) Heß, B. A.; Marian, C. M.; Wahlgren, U.; Gropen, O. A mean-field spin-orbit method applicable to correlated wavefunctions. *Chem. Phys. Lett.* **1996**, *251*, 365−371.
(40) Malmqvist, P.-Å.; Roos, B. O.; Schimmelpfennig, B. The restricted active space (RAS) state interaction approach with spin−orbit coupling. *Chem. Phys. Lett.* **2002**, *357*, 230−240.
(41) Swerts, B.; Chibotaru, L. F.; Lindh, R.; Seijo, L.; Barandiaran, Z.; Clima, S.; Pierloot, K.; Hendrickx, M. F. A. Embedding Fragment ab Initio Model Potentials in CASSCF/CASPT2 Calculations of Doped Solids: Implementation and Applications. *J. Chem. Theory. Comput.* **2008**, *4*, 586−594.

https://doi.org/10.1021/acs.inorgchem.2c00071
Inorg. Chem. 2022, 61, 5972−5976